Med Biol Eng Comput (2013) 51:233–242
DOI 10.1007/s11517-012-0954-0

ORIGINAL ARTICLE

# Deriving respiration from photoplethysmographic pulse width

**Jesús Lázaro · Eduardo Gil · Raquel Bailón · Ana Mincholé · Pablo Laguna**

Received: 2 May 2012 / Accepted: 8 August 2012 / Published online: 21 September 2012


**Abstract** A method for deriving respiration from the pulse photoplethysmographic (PPG) signal is presented. This method is based on the pulse width variability (PWV), and it exploits the respiratory information present in the pulse wave velocity and dispersion. It allows to estimate respiration signal from only a pulse oximeter which is a cheap and comfortable sensor. Evaluation is performed over a database containing electrocardiogram (ECG), blood pressure (BP), PPG, and respiratory signals simultaneously recorded in 17 subjects during a tilt table test. Respiratory rate estimation error is computed obtaining of $1.27 \pm 7.81$ % ($0.14 \pm 14.78$ mHz). For comparison purposes, we have also obtained a respiratory rate estimation from other known methods which involve ECG, BP, or also PPG signals. In addition, we have also combined respiratory information derived from different methods which involve only PPG signal, obtaining a respiratory rate error of $-0.17 \pm 6.67$ % ($-2.16 \pm 12.69$ mHz). The presented methods, PWV and combination of PPG derived respiration methods, avoid the need of ECG to derive respiration without degradation of the obtained estimates, so it is possible to have reliable respiration rate estimates from just the PPG signal.

J. Lázaro (✉) · E. Gil · R. Bailón · A. Mincholé · P. Laguna
Communications Technology Group (GTC), Aragón Institute of Engineering Research (I3A), IIS Aragón, Universidad de Zaragoza, Zaragoza, Spain
e-mail: jlazarop@unizar.es

J. Lázaro · E. Gil · R. Bailón · A. Mincholé · P. Laguna
Centro de Investigación Biomédica en Red en Bioingeniería, Biomateriales y Nanomedicina (CIBER-BBN), Zaragoza, Spain

**Keywords** Photoplethysmography · PPG-derived respiration · Respiratory frequency · Respiratory system · Robustness · Signal synthesis

## 1 Introduction

Obtaining accurate respiratory signal and rate from non-invasive devices is useful in several situations. The simple observation of respiratory rate remains the first and often the most sensitive marker of acute respiratory dysfunction [12]. There exist specific devices for monitoring respiration based on different techniques such as spirometry, pneumography or plethysmography, but those devices may interfere with natural breathing, and are inconvenient in certain applications such as ambulatory monitoring, stress testing, and sleep apnea diagnosis [2].

Many algorithms for deriving respiration from the electrocardiogram (ECG) have been developed. Several of them are reviewed in [1]. In [8], respiration is estimated from the amplitude of R peak in ECG, and subsequently it is visually compared with the respiratory signal recorded as reference by pneumographic techniques. In other studies such as [19] respiration estimation is accomplished from the area of each QRS complex in a fixed time window in two ECG leads, and compared visually with the reference respiratory signal. In [22] a very similar method is proposed, but evaluation is performed with a more analytic method. There also have been published studies in which the respiration estimation is accomplished from the electrical axis rotation angles obtained from ECG leads [2, 20].

There also exist studies in which respiration is estimated from the blood pressure (BP) signal, which also can be acquired by non-invasive techniques. In [6], the estimation is performed with an algorithm based on the variability of

the area enclosed under the dicrotic notch in BP signal. Another known method for non-invasive respiration estimation is the pulse transit time (PTT) signal [3], which is the time taken by the pulse wave to propagate from the heart to the periphery and its computation requires to use both ECG and pulse photoplethysmographic (PPG) signals.

Deriving respiration from PPG signal is especially interesting because it is provided by a cheap and very comfortable device called pulse oximeter, which is widely used in clinical routine for blood oxygen saturation measurement. It allows to know if a low oxygen saturation is due to low respiratory rates or is the result of a low degree of gas exchange in the lungs, which can represent a dangerous physiological condition [21]. Blood oxygen saturation is a very important parameter in studies concerning respiration and essential in many situations such as sleep apnea diagnosis. Obtaining accurate respiratory signal from a pulse oximeter would allow us to consider an ambulatory diagnosis with its both social and economic advantages. It is also interesting for sport trainings since it is useful to know the point when the exercise shifts from aerobic to anaerobic and that point is determined from the curve of respiratory rate and other parameters related to breathing among others [14]. The pulse oximeter can be placed at different parts of the body (i.e. fingers, ears) depending on the concrete application. There are several known methods for deriving respiration from the PPG signal such as pulse amplitude variability (PAV) [15] and pulse rate variability (PRV). Although PRV is not an exact surrogate for the heart rate variability (HRV) [4], both signals are highly correlated even during non-stationary conditions [10]. In that way, PRV is also affected by parasympathetic system and so related to respiration. In [5], both amplitude and frequency modulation of PPG signal due to respiration are used to compare two time–frequency methods for respiratory rate estimation.

A preliminary analysis of how respiration modulates the width of the pulses in PPG signal was presented in [17]. The study has now been extended and further elaborated, where the accuracy of the method is increased, and a comparison with other physiological signals and other similar methods in the literature is performed. Our hypothesis is that respiration affects pulse wave width: during inspiration sympathetic activation stiffs arteries increasing pulse wave velocity in comparison with expiration, moreover there are intrathoracic pressure variations induced by respiration whose effect can add to the former constructively. We also propose a method for combining the respiratory information carried by several PPG derived respiration (DR) signals based on [2]. Evaluation is performed over a database which contains simultaneous recordings of ECG, BP, PPG and respiration signals. For comparison, we also evaluate DR signals obtained with other methods which involve the ECG, PPG, and BP signals.

## 2 Methods

### 2.1 Data, signal preprocessing and significant points detection

The database was recorded during a tilt table test from 17 volunteers (11 men), aged 28.5 ± 2.5 years, according to the following protocol: 4 min in early supine position, 5 min tilted head-up to an angle of 70° and 4 min back to later supine position. Table takes 18 s to tilt during transitions. The PPG signal ($x_{\mathrm{PPG}}(n)$) was recorded from index finger by Biopac OXY100C with a sampling rate of 250 Hz (see an example in Fig. 1), whereas the standard ECG leads I, III and the six precordials were recorded by Biopac ECG100C with a sampling rate of 1,000 Hz, and the respiratory signal ($r(n)$, see an example in Fig. 2) was recorded with a sampling rate of 125 Hz by a plethysmography-based technique using Biopac RSP100C sensor and TSD201 transducer. Standard ECG lead II was obtained by the sum of I and III leads, and vectorcardiogram (VCG) was synthesized using the inverse Dower matrix [7]. The BP ($x_{\mathrm{BP}}(n)$) signal was recorded with a sampling rate of 250 Hz by Finometer system (see an example in Fig. 3).

The ECG baseline contamination was removed with a high-pass filter with a cutoff frequency of 0.03 Hz, and the 50 Hz interference was attenuated with the non-linear technique described in [13]. Then, location of each QRS in lead V4 ($n_{\mathrm{QRS}i}$) were obtained by the wavelet based QRS detector described in [18]. Lead V4 was chosen because of its high SNR and also because it is one of those whose amplitude modulation is in phase with respiration. Then, locations of each maximum of R wave ($n_{\mathrm{R}i}$) and minimum of S wave ($n_{\mathrm{S}i}$) (see Fig. 3) were detected by a search of maximum and subsequent minimum (respectively) within an 80-ms length time window centred at $n_{\mathrm{QRS}i}$. The

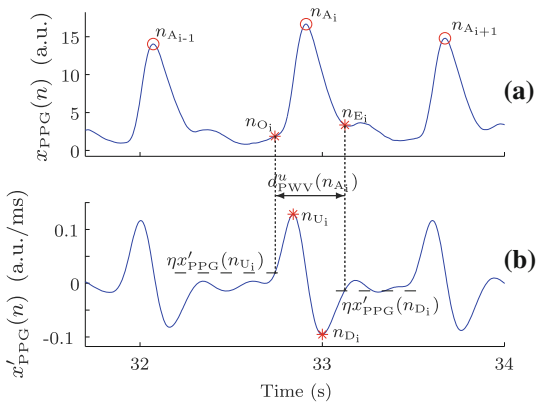


**Fig. 1** Example of $x_{\mathrm{PPG}}(n)$ (**a**) and its low-pass derivative $x'_{\mathrm{PPG}}(n)$ (**b**) with definitions of pulse onset ($n_{\mathrm{O}i}$) and end ($n_{\mathrm{E}i}$) points in PPG, and PWV based PPG DR signal

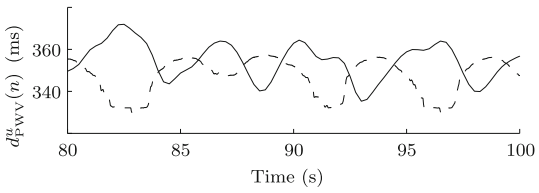


**Fig. 2** Example of $d^u_{PWV}(n)$ (*continuous line*) and amplitude scaled reference $r(n)$ (*dashed line*) for comparison

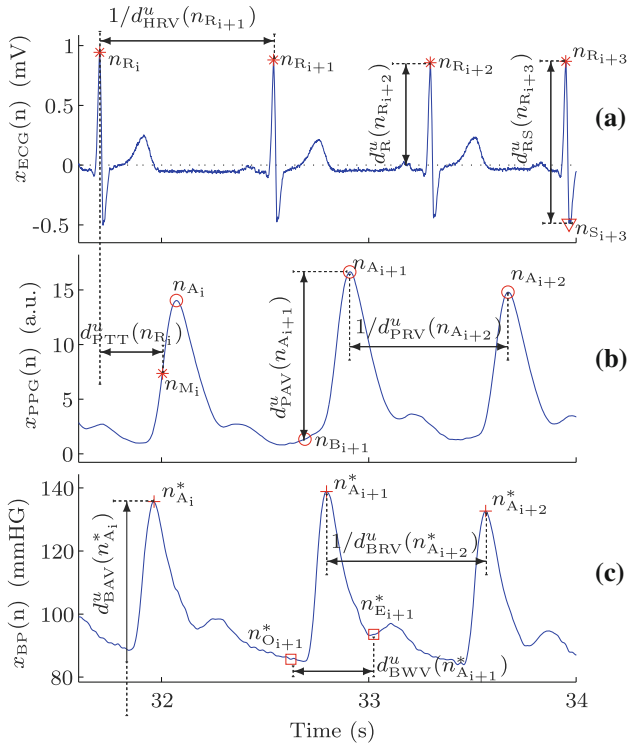


**Fig. 3** Examples of $x_{ECG}(n)$ (**a**), $x_{PPG}(n)$ (**b**), and $x_{BP}(n)$ (**c**), with definitions of ECG DR and BP DR signals, and definitions of PRV- and PAV-based PPG DR signals

preprocessing applied to the PPG and BP signals consists of a low-pass filtering with a cutoff frequency of 35 Hz. Subsequently, each pulse apex ($n_{Ai}$) and basal ($n_{Bi}$) points in PPG and each systolic pressure point ($n^*_{Ai}$) in BP (see Fig. 3) were automatically determined using the algorithm described in [9] which uses the $n_{Ri}$ previously obtained. Artifactual PPG pulses were suppressed by using the artefact detector described in [11].

## 2.2 Pulse width variability

In order to measure the pulses width in PPG signal, it is necessary to locate the onset and end of each pulse wave. The detection is performed with a modification of the algorithm presented in [16] which was originally designed for detecting the wave boundaries in ECG signals. The algorithm uses a low-pass derivative

$$x'_{PPG}(n) = x_{PPG_{LP}}(n) - x_{PPG_{LP}}(n-1) \tag{1}$$

where $x_{PPGLP}(n)$ is the low-pass filtered version of PPG signal, using a cut–off frequency of $f_C$ which was set to 5 Hz as shown in Sect. 3.1.

For the $i$th pulse wave, the algorithm uses the maximum upslope point ($n_{Ui}$)

$$n_{U_i} = \arg\max_n \{x'_{PPG}(n)\}, \quad n \in [n_{A_i} - 0.3f_s^P, n_{A_i}] \tag{2}$$

where $f_s^P$ is the sampling rate of the PPG signal.

The pulse wave onset $n_{Oi}$ search is limited to $\Omega_{O_i}$ interval:

$$\Omega_{O_i} = [n_{A_i} - 0.3f_s^P, n_{U_i}] \tag{3}$$

and is determined as:

$$n_{O_i} = \begin{cases} \arg\min_{n\in\Omega_{O_i}} \{|x'_{PPG}(n) - \eta x'_{PPG}(n_{U_i})|\} & \text{if } C_1 \\ \text{last relative minimum of } x'_{PPG}(n), & \text{if } C_2 \\ \arg\min_{n\in\Omega_{O_i}} \{x'_{PPG}(n)\}, & \text{otherwise} \end{cases} \tag{4}$$

where $\eta x'_{PPG}(n_{Ui})$ represents a beat varying threshold dependent on maximum upslope value of each pulse wave, and conditions $C_1$ and $C_2$ are defined by:

$$C_1 : \exists m \in \Omega_{O_i} \ni x'_{PPG}(m) \le \eta x'_{PPG}(n_{U_i})$$

$$C_2 : \overline{C_1} \wedge \text{exists a relative minimum of } x'_{PPG}(n) \text{ in } \Omega_{O_i}.$$

Pulse wave ends $n_{Ei}$ were detected in a similar way as $n_{Oi}$ but using maximum downslope ($n_{Di}$) instead of $n_{Ui}$, in the interval $[n_{Ai}, n_{Ai} + 0.3f_s^P]$ and $\Omega_{E_i} = [n_{D_i}, n_{A_i} + 0.3f_s^P]$. Figure 1 illustrates the significant points determination rule of this algorithm.

Once $n_{Oi}$ and $n_{Ei}$ are detected, we can compute a DR signal based on pulse width variability (PWV) as:

$$d^u_{PWV}(n) = \sum_i \frac{1}{f_s^P}(n_{E_i} - n_{O_i})\delta(n - n_{A_i}) \tag{5}$$

where the superscript "$u$" denotes that the signal is unevenly sampled. Figure 1 illustrates this definition and Fig. 2 shows an example of this DR signal where it becomes evident the close relation of temporal oscillations of this signal to those of respiration signal $r(n)$.

## 2.3 Other derived respiration signals

As mentioned previously, for comparison purposes, respiration has also been derived by other known methods which involve the ECG, BP, and PPG signals. Studied DR

signals from PPG are three: PRV, PAV, and the PWV already presented.

The one based on PRV is defined as:

$$d^{u}_{\mathrm{PRV}}(n) = \sum_i f_{\mathrm{s}}^{\mathrm{P}} \frac{1}{n_{\mathrm{A}_i} - n_{\mathrm{A}_{i-1}}} \delta(n - n_{\mathrm{A}_i}). \tag{6}$$

The PAV-based DR signal takes its reference to derive amplitude at the basal point:

$$d^{u}_{\mathrm{PAV}}(n) = \sum_i [x_{\mathrm{PPG}}(n_{\mathrm{A}_i}) - x_{\mathrm{PPG}}(n_{\mathrm{B}_i})] \delta(n - n_{\mathrm{A}_i}). \tag{7}$$

From the ECG, we have obtained six DR signals: one based on HRV, two based on R amplitude variability, and three based on the electrical axis rotation angles called $d^{u}_{\Phi_X}(n), d^{u}_{\Phi_Y}(n)$ and $d^{u}_{\Phi_Z}(n)$, which are computed by the same algorithm presented in [2] based on spatio-temporal alignment of successive QRS–VCG loops with respect to a reference loop.

The HRV-based DR signal is computed similar to the PRV-based one:

$$d^{u}_{\mathrm{HRV}}(n) = \sum_i f_{\mathrm{s}}^{\mathrm{E}} \frac{1}{n_{\mathrm{R}_i} - n_{\mathrm{R}_{i-1}}} \delta(n - n_{\mathrm{R}_i}) \tag{8}$$

where $f_{\mathrm{s}}^{\mathrm{E}}$ is the sampling rate of the ECG signal.

The difference of two R wave amplitude-based DR signals is the reference used to derive signal amplitude: one takes the reference as zero while the other one takes it as the amplitude of S point at the same beat:

$$d^{u}_{\mathrm{R}}(n) = \sum_i x_{\mathrm{ECG}}(n_{\mathrm{R}_i}) \delta(n - n_{\mathrm{R}_i}) \tag{9}$$

$$d^{u}_{\mathrm{RS}}(n) = \sum_i [x_{\mathrm{ECG}}(n_{\mathrm{R}_i}) - x_{\mathrm{ECG}}(n_{\mathrm{S}_i})] \delta(n - n_{\mathrm{R}_i}) \tag{10}$$

where $x_{\mathrm{ECG}}(n)$ is the filtered ECG at lead V4.

Another method which involves the ECG derives respiration from PTT. We have obtained the PTT signal and taken it as a DR signal:

$$d^{u}_{\mathrm{PTT}}(n) = \frac{1}{f_{\mathrm{s}}^{\mathrm{P}}} \left( n_{\mathrm{M}_i} - \frac{f_{\mathrm{s}}^{\mathrm{P}}}{f_{\mathrm{s}}^{\mathrm{E}}} n_{\mathrm{R}_i} \right) \delta(n - n_{\mathrm{R}_i}) \tag{11}$$

where the $f_{\mathrm{s}}^{\mathrm{P}} / f_{\mathrm{s}}^{\mathrm{E}}$ term is due to the different sampling rates of ECG and PPG signals, and $n_{\mathrm{M}i}$ is the time instant when the PPG signal reaches 50 % of amplitude between onset and apex points:

$$n_{\mathrm{M}_i} = \underset{n \in [n_{\mathrm{O}_i}, n_{\mathrm{A}_i}]}{\arg\min} \left\{ \left| x_{\mathrm{PPG}}(n) - \frac{x_{\mathrm{PPG}}(n_{\mathrm{O}_i}) + x_{\mathrm{PPG}}(n_{\mathrm{A}_i})}{2} \right| \right\}. \tag{12}$$

Since PPG measures the pulse wave caused by periodic pulsations in arterial blood volume and BP depends, among other factors, on this blood volume, we have obtained a DR signal based on BP pulses width as in PPG:

$$d^{u}_{\mathrm{BWV}}(n) = \sum_i \frac{1}{f_{\mathrm{s}}^{\mathrm{P}}} (n^{*}_{\mathrm{E}_i} - n^{*}_{\mathrm{O}_i}) \delta(n - n^{*}_{\mathrm{A}_i}) \tag{13}$$

where $n^{*}_{\mathrm{O}_i}$ and $n^{*}_{\mathrm{E}_i}$ are the onset and end points of the $i$th pressure wave in BP (see Fig. 3) detected with the same algorithm used for the PPG signal.

We have obtained also other two BP DR signals: BP rate variability (BRV) $d^{\mathrm{P}}_{\mathrm{s}}(n)$ and BP amplitude variability (BAV) $d^{u}_{\mathrm{BAV}}(n)$. The first one, defined in (14), is based on rate similarly to $d_{\mathrm{PRV}}(n)$ and $d_{\mathrm{HRV}}(n)$, and the second one is based on the beat-to-beat systolic pressure variability as defined in (15).

$$d^{u}_{\mathrm{BRV}}(n) = \sum_i f_{\mathrm{s}}^{\mathrm{P}} \frac{1}{n^{*}_{\mathrm{A}_i} - n^{*}_{\mathrm{A}_{i-1}}} \delta(n - n^{*}_{\mathrm{A}_i}) \tag{14}$$

$$d^{u}_{\mathrm{BAV}}(n) = \sum_i x_{\mathrm{BP}}\left(n^{*}_{\mathrm{A}_i}\right) \delta\left(n - n^{*}_{\mathrm{A}_i}\right). \tag{15}$$

Note that in $d^{u}_{\mathrm{BAV}}(n)$ the absolute value of systolic pressure is considered, instead of referring it to the basal point as in $d^{u}_{\mathrm{PAV}}(n)$, since, otherwise, respiratory modulation of systolic and diastolic pressures could compensate each other.

Figure 3 illustrates definitions of all DR signals defined in this section, and Fig. 4 shows an example of the unevenly sampled version of each DR signal. Due to the presence of some outliers in the DR signals, we applied a median absolute deviation (MAD)-based outlier rejection rule as described in [2]. Finally, we obtained a 4-Hz evenly sampled version of each DR signal by cubic splines interpolation, and filtered with a band-pass filter (0.075–1 Hz). The resulting signals are denoted without the superscript "$u$", i.e., $d_{\mathrm{PWV}}(n)$ is the 4-Hz, outlier-rejected, evenly sampled, band-pass filtered version of $d^{u}_{\mathrm{PWV}}(n)$.

### 2.4 Respiratory rate estimation

The respiratory rate estimation algorithm is based on the one presented in [2]. It allows to estimate the respiratory rate from up to $N$ DR signals, combining them in order to increase robustness.

For power spectrum estimation, we used the Welch periodogram. As in [2], running power spectra of each DR signal used in combination are averaged in order to reduce the variance. For the $j$th DR signal and $k$th running interval of $T_{\mathrm{s}}$-s length, the power spectrum $S_{j,k}(f)$ results from averaging the power spectra obtained from subintervals of length $T_{\mathrm{m}}$ s ($T_{\mathrm{m}} < T_{\mathrm{s}}$) using an overlap of $T_{\mathrm{m}}/2$ s, after a power normalization in [0, 1] Hz band. A $T_{\mathrm{s}}$-s spectrum is estimated every $t_{\mathrm{s}}$ s.

For each $S_{j,k}(f)$, the location of largest peak $f^{\mathrm{P}}_{\mathrm{s}}(j, k)$ is detected. Then, a reference interval $\Omega_{\mathrm{R}}(k)$ is established as:

$$\Omega_{\mathrm{R}}(k) = [f_{\mathrm{R}}(k-1) - \delta, f_{\mathrm{R}}(k-1) + 2\delta] \tag{16}$$

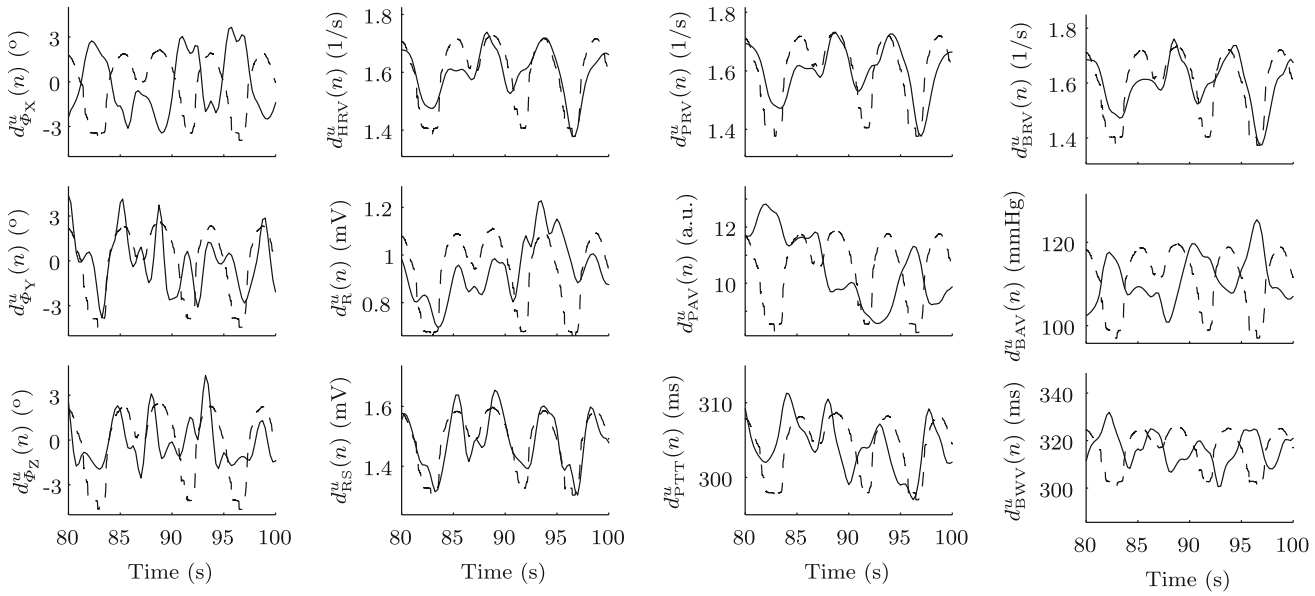


**Fig. 4** An example of unevenly sampled version of each derived respiration signal (*continuous line*) and amplitude-scaled reference $r(n)$ (*dashed line*) for comparison

where $f_R(k-1)$ is a respiratory frequency reference obtained from previous $(k-1)$ steps and defines the location of $\Omega_R(k).\Omega_R(k)$ is asymmetric with respect to $f_R(k-1)$ because the most important contamination present in power spectra is in the low frequency (LF) band due to the sympathetic system activity, reflected at some DR signals.

All peaks larger than 85 % of $f_p^I(j,k)$ inside $\Omega_R(k)$ are detected, and $f_p^{II}(j,k)$ is chosen as the nearest to $f_R(k-1)$. Note that $f_p^{II}(j,k)$ can be the same $f_p^I(j,k)$ if the largest peak is also the nearest to $f_R(k-1)$. Then, $L_s$ spectra $S_{j,k}(f)$ are "peak-conditioned" averaged; only those $S_{j,k}(f)$ which are sufficiently peaked take part in the averaging. In this paper, "peaked" denotes that $f_p^{II}(j,k)$ exists and a certain percentage $(\xi)$ of the spectral power must be contained in an interval centered around it. Peak-conditioned averaging is defined as:

$$\bar{S}_k(f) = \sum_{l=0}^{L_s-1} \sum_j \chi^A_{j,k-l} \chi^B_{j,k-l} S_{j,k-l}(f) \tag{17}$$

where $\chi^A_{j,k-l}$ and $\chi^B_{j,k-l}$ represent two criteria aimed at deciding whether power spectrum $S_{j,k-l}(f)$ is peaked enough or not, preventing those not peaked enough spectra from taking part in the average. On one hand, $\chi^A$ lets those spectra whose peakness is greater than a fixed value take part in the average, as shows (18), and on the other hand, $\chi^B$ compares the spectra of different DR signals, letting those spectra more peaked in each time instant take part in the average, although all of them have passed the $\chi^A$ criterion, as shows (19). Note that $\chi^B$ has no effect if the estimation is being accomplished from only one DR signal $(N=1)$.

$$\chi^A_{j,k} = \begin{cases} 1, & P_{j,k} \geq \xi \\ 0, & \text{otherwise} \end{cases} \tag{18}$$

$$\chi^B_{j,k} = \begin{cases} 1, & P_{j,k} \geq \max_j \{P_{j,k}\} - \lambda \\ 0, & \text{otherwise} \end{cases} \tag{19}$$

where $P_{j,k}$ is defined by

$$P_{j,k} = \frac{\int_{\max\{f_p^{II}(j,k)-0.6\delta,\, f_R(k-1)-\delta\}}^{\min\{f_p^{II}(j,k)+0.6\delta,\, f_R(k-1)+2\delta\}} S_{j,k}(f)\mathrm{d}f}{\int_{f_R(k-1)-\delta}^{f_R(k-1)+2\delta} S_{j,k}(f)\mathrm{d}f}. \tag{20}$$

In the averaged spectrum $\bar{S}_k(f)$ the algorithm also searches the largest peak (denoted $f^P_{s\,p}(k)$) and $f^{II}_{a\,p(k)}$ defined as the nearest to $f_R(k-1)$ inside the interval $\Omega_R(k)$ which is at least larger than 85 % of $f^I_{ap(k)}$. At this time the reference frequency $f_R(k)$ can be updated as:

$$f_R(k) = \beta f_R(k-1) + (1-\beta) f_p(k) \tag{21}$$

where $\beta$ denotes the forgetting factor and $f_p(k)$ is defined by

$$f_p(k) = \begin{cases} f^{II}_{a_{p(k)}}, & \exists f^{II}_{a_p(k)} \\ f^{I_a}_p(k), & \text{otherwise} \end{cases}. \tag{22}$$

Finally, estimated respiration rate $\hat{f}(k)$ is defined as:

$$\hat{f}(k) = \alpha \hat{f}(k-1) + (1-\alpha) f_p(k) \tag{23}$$

$$\alpha = \begin{cases} \alpha_2, & \exists f^{II_a}_p(k) \\ \alpha_1, & \text{otherwise} \end{cases}. \tag{24}$$

where $\alpha_2 \leq \alpha_1$, providing more memory when $f^{\mathrm{II}}_{\mathrm{a\,p}(k)}$ could not be set.

Note that $\bar{S}_k(f)$ is the result of an average from zero up to $N \times L_s$ power spectra. If no spectrum takes part in the average, the algorithm increases the reference interval by doubling the $\delta$ value and repeat the process from the search of $f^{\mathrm{I}}_{\mathrm{p}}(j, k)$ and $f^{\mathrm{II}}_{\mathrm{p}}(j, k)$ in individual power spectra. In the case that no spectrum is peaked enough after this second iteration, $f_{\mathrm{R}}(k)$ and $\hat{f}(k)$ are set as previous $f_{\mathrm{R}}(k-1)$ and $\hat{f}(k-1)$, respectively.

At initialization time, in order to reduce the risk of spurious frequency selection, $\delta$ is set to 0.125 Hz and $f_{\mathrm{R}}(0)$ is set to 0.275 Hz, allowing the algorithm to pick peaks inside [0.15, 0.525] Hz band. Occasionally, respiratory rate can be below 0.15 Hz so algorithm could not be initialized as proposed. To deal with that issue, if $f_{\mathrm{R}}(k)$ is not set after 5 averages $\bar{S}_k(f)$, then $\delta$ is increased allowing algorithm to pick peaks in full [0, 1] Hz studied band.

Concatenation of all $\bar{S}_k(f)$ results in a time–frequency map $\bar{S}(k,f)$ where the LF contamination is considerably reduced, as shown in Fig. 5. Values for $L_s$, $T_s$, and $T_m$ were selected as in [2]; 5, 40, and 12 s, respectively. The other parameters were empirically set for this work:

- $\xi = 0.4$ and $\lambda = 0.05$ are based on the observation of spectra to achieve a good compromise for peak spectrum acceptance/rejection.
- $\beta = 0.8$ is slightly higher than 0.7 used in [2] for stress test data, since in regular conditions respiratory frequency band is expected to change more gradually than in stress test. Thus, a higher filtering for $f_{\mathrm{R}}$ tracking has shown to be more adequate in this work.
- $\delta = 0.08$ Hz is selected according to the typical width of expected band where respiration peak is supposed to be located, which is taken as 0.24 Hz (the typical HF bandwidth).
- $\alpha_2 = 0.3$ is taken by fixing the maximum allowed changes in respiratory frequency inside the frequency band. This filtering is much lower than the one imposed for the frequency band by $\beta$ since within the respiratory band higher sudden changes of the respiratory frequency are observed and so they are preserved.
- $\alpha_1 = 0.7$ which represents a high memory when $\hat{f}$ is far from $f_{\mathrm{R}}$, outside $\Omega_{\mathrm{R}}$.

### 2.5 Performance measurements

With the objective of evaluating the different methods for deriving respiration, we obtained a 4-Hz sampled,

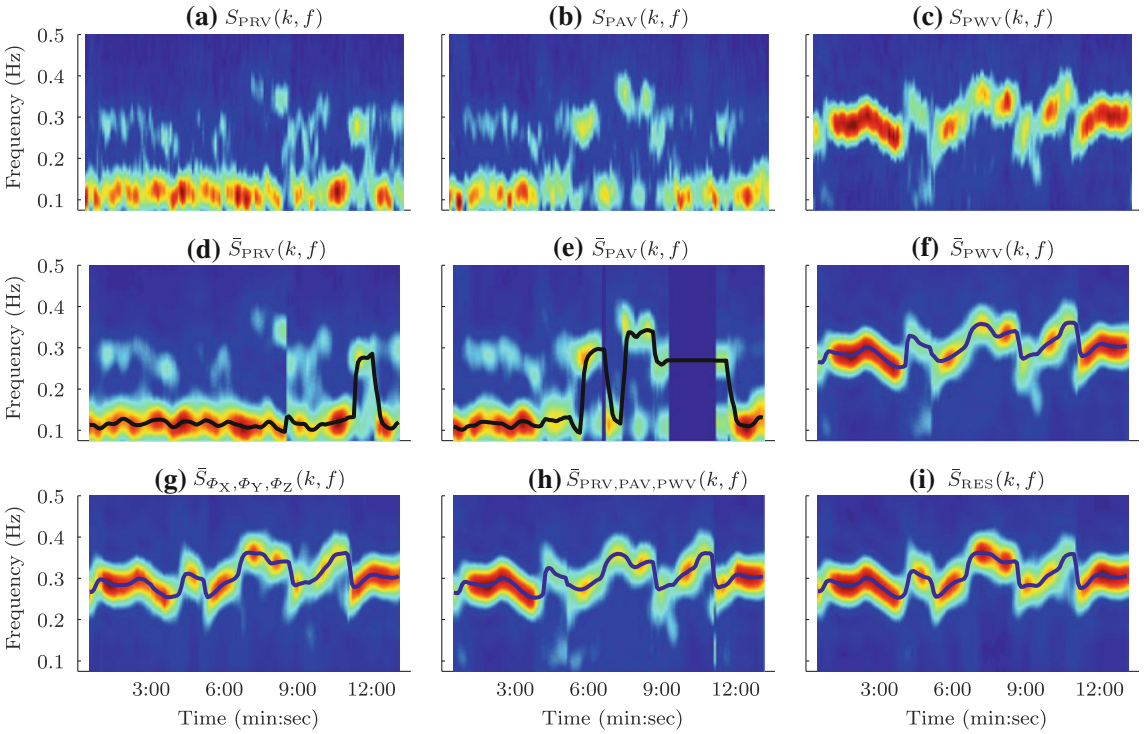


**Fig. 5** Examples of time–frequency maps: Welch periodograms for PRV (**a**), PAV (**b**), and PWV (**c**); peak-conditioned average with estimated rate in *black line* for PRV (**d**), PAV (**e**), PWV (**f**), combination of $\Phi_{\mathrm{X}}, \Phi_{\mathrm{Y}}$ and $\Phi_{\mathrm{Z}}$ (**g**), combination of PRV, PAV and PWV (**h**), and reference respiratory signal (**i**)

band-pass filtered, [0.075, 1] Hz version of the respiratory signal $r(n)$, and we computed two error functions for each one of the 17 subjects in our database: absolute error $e_A(k)$ and relative error $e_R(k)$:

$$e_A(k) = \hat{f}_d(k) - \hat{f}_{RES}(k) \quad (25)$$

$$e_R(k) = \frac{e_A(k)}{\hat{f}_{RES}(k)} \times 100 \quad (26)$$

where $\hat{f}_d(k)$ and $\hat{f}_{RES}(k)$ are the respiratory rates estimated from the evaluated DR signal and $r(n)$, respectively. Note that the same absolute differences can correspond to very different relative errors due to the $\hat{f}_{RES}(k)$ normalization.

In order to study the optimal values for parameters $\eta$ and $f_C$ in the pulse width-based DR signals, the performance measurement $z$ was defined as the intersubject mean of intrasubject mean of the absolute value of relative error $|e_R(k)|$:

$$z = \frac{1}{M}\sum_{m=1}^{M} \overline{|e_R(k)|}_m \quad (27)$$

where $M$ is the number of subjects in our database, and $\overline{|e_R(k)|}_m$ is the mean of $|e_R(k)|$ obtained from $m$th subject.

## 3 Results

### 3.1 Pulse width measurement parameters optimization

In reference to the parameters optimization of the pulse width measurement algorithm, we computed all the 286 possible combinations corresponding to $\eta \in [0, 0.5]$ with a step of 0.05, and $f_C \in [2.5, 15]$ Hz with a step of 0.5 Hz, for both PPG and BP signals. The values which minimized $z$ were $\eta = 0.05$ and $f_C = 5$ Hz for PPG signal (with $z = 5.26$ %), and $\eta = 0.3$ and $f_C = 3$ Hz for BP signal (with $z = 5.66$ %).

We used these optimal values to obtain DR signals based on width ($d_s^P(n)$) and $d_{BWV}^{\mu}(n)$).

### 3.2 Evaluation of derived respiration signals

In order to evaluate the DR signals, we computed the mean and standard deviation of both $e_R(k)$ and $e_A(k)$ signals for each subject. Then, intersubject mean of both means and standard deviations (STD) were computed for three groups of subjects: one group containing all the subjects, and other two groups which make a division of the subjects based on whether their mean respiratory rate $\bar{f}_{RES}$ is greater than 0.15 Hz or not. In other words, whether their $\bar{f}_{RES}$ overlaps in frequency with the sympathetic modulation or not. Respiratory rate was estimated from each DR signal but for rotation angle series, and from two combinations: one combining all three PPG DR signals $P_{COMB}$, and other combining all three rotation angle series $\Phi_{COMB}$. Results are shown in Table 1. Moreover, the percentage of times in which each DR signal is used in $P_{COMB}$ is shown in Table 2.

For comparison with [5], we also obtained the median of $e_R(k)$ for each subject for our two proposed methods: the PWV and the combination of PRV, PAV and PWV, $P_{COMB}$. Table 3 shows inter-subject median and inter-quartile range (IQR) of these medians, for the same three groups of subjects over which we computed the mean of means and STD.

## 4 Discussion

As it was mentioned previously, deriving respiration from the PPG signal is especially interesting because it is recorded by a simple and cheap device which also result very comfortable for the patient and, in addition, is widely adopted as a blood oxygen saturation monitor: the pulse oximeter. Blood oxygen saturation is a very important parameter in studies concerning respiration and essential in many situations such as sleep apnea diagnosis. Obtaining accurate respiratory signal from a pulse oximeter would allow us to consider an ambulatory diagnosis with its both social and economic advantages.

We have developed a method for deriving respiration from the PPG signal: the PWV, which has obtained very accurate results, comparable or even better than other known methods which involve ECG or BP.

In respiratory rate estimation from only one DR signal, this method based on PWV has obtained the best results ($1.27 \pm 7.81$%; $0.14 \pm 14.78$ mHz), being much better than PRV ($-10.29 \pm 13.63$ %; $-34.60 \pm 33.73$ mHz) or PAV ($-8.75 \pm 17.06$ %; $-26.41 \pm 41.84$ mHz), which are more affected by the sympathetic modulation which results in a very high negative error in the $\bar{f}_{RES} \geq 0.15$ Hz group. The PWV-based method results are also comparable to the PTT-based one ($0.96 \pm 9.26$ %; $-1.54 \pm 18.57$ mHz), which needs ECG in addition to PPG signal.

In $P_{COMB}$, the PWV-based method has a fundamental role since PWV is much less affected by the sympathetic modulation (see Fig. 5). This fact explains why the PWV method is more often used in the $\bar{f}_{RES} \geq 0.15$ Hz group (67.63 % of times) than in the $\bar{f}_{RES} < 0.15$ Hz group (42.41 % of times) (Table 2). Results referred to estimated rate from $P_{COMB}$ ($-0.17 \pm 6.67$ %; $-2.16 \pm 12.69$ mHz) are comparable with combination of three electrical axis rotation angle series ($2.05 \pm 6.92$ %; $2.63 \pm 11.50$ mHz) and have outperformed those obtained with only PWV. This means it is reasonable to combine respiratory

**Table 1** Inter-subject mean of means and standard deviations of $e_A(k)$ in mHz and $e_R(k)$ in percentage

| | $\bar{f}_{RES} \geq 0.15$ Hz | | $\bar{f}_{RES} < 0.15$ Hz | | All | |
|---|---|---|---|---|---|---|
| | $e_A(k)$ (mHz) | [$e_R(k)$ (%)] | $e_A(k)$ (mHz) | [$e_R(k)$ (%)] | $e_A(k)$ (mHz) | [$e_R(k)$ (%)] |
| ECG methods | | | | | | |
| HRV | | | | | | |
| Mean | −62.78 | (−21.21) | 4.08 | (4.19) | −39.18 | (−12.25) |
| STD | 46.31 | (15.15) | 13.75 | (11.91) | 34.82 | (14.00) |
| R | | | | | | |
| Mean | −24.33 | (−7.55) | 13.86 | (12.49) | −10.85 | (−0.48) |
| STD | 43.17 | (15.48) | 24.64 | (20.50) | 36.63 | (17.25) |
| RS | | | | | | |
| Mean | 6.28 | (3.04) | 40.28 | (41.50) | 18.28 | (14.84) |
| STD | 31.53 | (12.50) | 36.46 | (36.94) | 35.05 | (21.13) |
| $\Phi_{COMB}$ | | | | | | |
| Mean | 1.50 | (0.81) | 4.71 | (13.30) | 2.63 | (2.05) |
| STD | 10.52 | (4.58) | 4.31 | (11.20) | 11.50 | (6.92) |
| BP methods | | | | | | |
| BRV | | | | | | |
| Mean | −58.13 | (−19.21) | 4.71 | (4.31) | −35.95 | (−10.78) |
| STD | 44.06 | (14.49) | 13.30 | (11.20) | 33.33 | (13.62) |
| BAV | | | | | | |
| Mean | −14.68 | (−4.49) | 0.93 | (1.28) | −9.17 | (−2.78) |
| STD | 34.63 | (11.80) | 13.14 | (10.66) | 24.04 | (11.40) |
| BWV | | | | | | |
| Mean | −2.01 | (−0.58) | 9.16 | (8.26) | 1.93 | (2.54) |
| STD | 12.94 | (4.82) | 19.01 | (15.97) | 15.08 | (8.76) |
| PPG methods | | | | | | |
| PRV | | | | | | |
| Mean | −55.89 | (−18.34) | 4.41 | (4.46) | −34.60 | (−10.29) |
| STD | 44.58 | (14.56) | 13.85 | (11.93) | 33.73 | (13.63) |
| PAV | | | | | | |
| Mean | −40.43 | (56.37) | −0.73 | (0.35) | −26.41 | (−8.75) |
| STD | −13.72 | (19.68) | 15.20 | (12.27) | 41.84 | (17.06) |
| PWV | | | | | | |
| Mean | −2.97 | (−0.92) | 5.85 | (5.32) | 0.14 | (1.27) |
| STD | 14.08 | (4.83) | 16.06 | (13.27) | 14.78 | (7.81) |
| $P_{COMB}$ | | | | | | |
| Mean | −4.35 | (−1.50) | 1.87 | (2.27) | −2.16 | (−0.17) |
| STD | 12.76 | (4.58) | 12.57 | (10.50) | 12.69 | (6.67) |
| Other methods | | | | | | |
| PTT | | | | | | |
| Mean | −5.76 | (−1.73) | 6.20 | (5.88) | −1.54 | (0.96) |
| STD | 20.21 | (6.89) | 15.58 | (13.62) | 18.57 | (9.26) |

$\Phi_{COMB}$ refers to the combination of the three rotation angle series, and $P_{COMB}$ refers to the combination of PRV, PAV, and PWV

information of these three signals or, in other words, the respiratory information carried by these three signals can complement.

The BWV-based method also obtained very good results ($2.54 \pm 8.76$ %; $1.93 \pm 15.08$ mHz), but acquiring BP signal is more uncomfortable and expensive than acquiring

**Table 2** Percentage of utilization of each DR signal in combination of PRV, PAV and PWV

| Group | Percentage of use | | |
|---|---|---|---|
| | PRV | PAV | PWV |
| $\bar{f}_{RES} \geq 0.15$ Hz | 48.24 | 37.80 | 67.63 |
| $\bar{f}_{RES} < 0.15$ Hz | 59.77 | 61.27 | 42.41 |
| All | 52.31 | 46.08 | 58.73 |

**Table 3** Inter–subject median and IQR of medians of $e_R(k)$ in percentage referent to PWV and combination of PRV, PAV and PWV

| Group | $e_R(k)$ (%) | | | |
|---|---|---|---|---|
| | PWV | | $P_{COMB}$ | |
| | Median | IQR | Median | IQR |
| $\bar{f}_{RES} \geq 0.15$ Hz | −0.24 | 0.48 | −0.67 | 0.41 |
| $\bar{f}_{RES} < 0.15$ Hz | 1.72 | 1.60 | 0.31 | 0.69 |
| All | 0.02 | 1.48 | −0.37 | 0.66 |

PPG signal and the first one provides no information about blood oxygen saturation.

The obtained values of median and IQR of medians ($0.02 \pm 1.48$ % for PWV and $-0.37 \pm 0.66$ % for $P_{COMB}$) are worse than those obtained in [5] ($\bar{f}_{RES}$ between 0.2 and 0.3 Hz, $0.00 \pm 0.00$ %; $\bar{f}_{RES}$ between 0.4 and 0.6 Hz, $0.00 \pm 1.18$ % for supine position and $0.00 \pm 1.07$ % for tilt position), but it must be kept in mind that database used in [5] contains signals recorded during a controlled respiration experiment. Controlled respiration means the subjects are instructed to breathe according to a timed beeping sound, generating known respiratory rates which provides a much better reference than ours. Moreover, those generated rates were constant, so estimation methods were not required to follow rate variations which is not an easy task and, furthermore, all generated rates were higher than 0.2 Hz, not overlapping in frequency with the sympathetic modulation present below 0.15 Hz in LF band.

Note the same subjects used to evaluate performance of the methods were also used to optimize the parameters $\eta$ and $f_c$, and this could bias the results. An additional test was performed: eight randomly selected subjects (training set) were used for parameters optimization and the remaining nine subjects (test set) were used for the evaluation of PWV and $P_{COMB}$ methods. Same values were obtained for optimal parameters ($\eta = 0.05$ and $f_c = 5$ Hz). Results were almost identical to the ones just commented above (see Table 1), obtaining a mean ± SD of frequency estimation error of $1.71 \pm 7.99$ % ($0.91 \pm 13.74$ mHz) for the PWV method, and $0.09 \pm 6.61$ % ($-1.75 \pm 12.26$ mHz) for the $P_{COMB}$ method.

The innovative method based on PWV represents a powerful approach for respiration estimation from the PPG signal. It showed better performance than other single DR signals in respiratory rate error terms ($1.27 \pm 7.81$ %). Additionally, using it in combination with PRV and PAV DR signals results improved to ($-0.17 \pm 6.67$ %) even outperforming the ones obtained with other methods which involve ECG or BP registration. These results allow to derive respiration from PPG suitable for ambulatory analysis and for sleep apnea diagnosis due to the simplicity of PPG recordings.

**Acknowledgments** This work is supported by Universidad de Zaragoza under fellowship PTAUZ-2011-TEC-A-003, Ministerio de Ciencia y Tecnología, Spain, FEDER; under project TEC2010-21703-C03-02, by CIBER-BBN through Instituto de Salud Carlos III, by ARAID and Ibercaja under Programa de APOYO A LA I+D+i and by Grupo Consolidado GTC from DGA.

## References

1. Bailón R, Sörnmo L, Laguna P (2006) ECG-derived respiratory frequency estimation. In: Clifford G, Azuaje F, McSharry P (eds) Advanced methods and tools for ECG data analysis. Artech House Inc., Boston, pp 215–244
2. Bailón R, Sörnmo L, Laguna P (2006) A robust method for ECG-based estimation of the respiratory frequency during stress testing. IEEE Trans Biomed Eng 53(7):1273–1285
3. Chua CP, Heneghan C (2005) Pulse transit time-derived respiratory parameters and their variability across sleep stages. Eng Med Biol Soc 27:6153–6156
4. Constant I, Laude D, Murat I, Elghozi J (1999) Pulse rate variability is not a surrogate for heart rate variability. Clin Sci 97(4): 391–397
5. Dash S, Shelley KH, Silverman DG, Chon KH (2010) Estimation of respiratory rate from ECG, photoplethysmogram, and piezoelectric pulse transducer signals: a comparative study of time–frequency methods. IEEE Trans Biomed Eng 57(5):1099–1107
6. De Meersman RE, Zion AS, Teitelbaum S, Weir JP, Liberman J, Downey J (1996) Deriving respiration from pulse wave: a new signal-processing technique. Am J Physiol Heart Circ Physiol 270(5):H1672–H1675
7. Edenbrant L, Pahlm O (1988) Vectorcardiogram synthesized from a 12-lead ECG; superiority of the inverse dower matrix. J Electrocardiol 21(4):361–367
8. Felblinger J, Boesch C (1997) Amplitude demodulation of the electrocardiogram signal (ECG) for respiration monitoring and compensation during MR examinations. Magn Reson Med 38(1):129–136
9. Gil E, Bailón R, Vergara JM, Laguna P (2010) PTT variability for discrimination of sleep apnea related decreases in the amplitude fluctuations of ppg signal in children. IEEE Trans Biomed Eng 57(5):1079–1088
10. Gil E, Orini M, Bailón R, Vergara J, Mainardi L, Laguna P (2010) Photoplethysmography pulse rate as a surrogate measurement of heart rate variability during non-stationary conditions. Physiol Meas 31:1271–1290
11. Gil E, Vergara JM, Laguna P (2008) Detection of decreases in the amplitude fluctuation of pulse photoplethysmography signal as indication of obstructive sleep apnea syndrome in children. Biomed Signal Process Control 3:267–277

12. Gravelyn TR, Weg JG (1980) Respiratory rate as an indicator of acute respiratory dysfunction. J Am Med Assoc 244(10):1123–1125
13. Hamilton PS (1996) A comparison of adaptive and nonadaptive filters for the reduction of powerline interference in the ecg. IEEE Trans Biomed Eng 43:105–109
14. James NW, Adams GM, Wilson AF (1989) Determination of anaerobic threshold by ventilatory frequency. Int J Sports Med 10(3):192–196
15. Johansson A, Oberg PA (1999) Estimation of respiratory volumes from the photoplethysmographic signal. Part I: experimental results. Med Biol Eng Comput 37:42–47
16. Laguna P, Jané R, Caminal P (1994) Automatic detection of wave boundaries in multilead ECG signals: validation with the CSE database. Comput Biomed Res 27:45–60
17. Lazaro J, Gil E, Bailón R, Laguna P (2011) Deriving respiration from the pulse photoplethysmographic signal. In: Computing in cardiology 2011. IEEE Computer Society Press, pp 713–716
18. Martinez JP, Almeida R, Olmos S, Rocha AP, Laguna P (2004) A wavelet-based ECG delineator: evaluation on standard databases. IEEE Trans Biomed Eng 51(4):570–581
19. Moody GB, Mark RG, Zoccula A, Mantero S (1986) Derivation of respiratory signals from multi-lead ECGs. In: Computers in cardiology 1985, IEEE Computer Society Press, pp 113–116
20. Travaglini A, Lamberti C, DeBie J, Ferri M (1999) Respiratory signal derived from eight-lead ECG. In: Computers in cardiology 1997, IEEE Computer Society Press, pp 65–68
21. Yang B, Chon K (2010) A novel approach to monitor non-stationary dynamics in physiological signals: application to blood pressure, pulse oximeter, and respiratory data. Ann Biomed Eng 38(11):3478–3488
22. Zhao L, Reisman S, Findly T (1994) Derivation of respiration from electrocardiogram during heart rate variability studies. In: Computers in cardiology 1993, IEEE Computer Society Press, pp 53–56

Med Biol Eng Comput (2013) 51:243
DOI 10.1007/s11517-012-0997-2

ERRATUM

# Erratum to: Deriving respiration from photoplethysmographic pulse width

**Jesús Lázaro · Eduardo Gil · Raquel Bailón · Ana Mincholé · Pablo Laguna**

Published online: 15 December 2012


**Erratum to: Med Biol Eng Comput**
**DOI 10.1007/s11517-012-0954-0**

Due to an equations formatting error, the presentation of some expressions was incorrect. A list of these expressions is given below:

Sect. 2.3, ninth paragraph: $d_{\mathrm{s}}^{\mathrm{P}}(n)$ should be read as $d_{\mathrm{BRV}}^{u}(n)$.

Sect. 3.1, second paragraph: $d_{\mathrm{s}}^{\mathrm{P}}(n)$ should be read as $d_{\mathrm{PWV}}^{u}(n)$.

Table 2: The correct table is given at the end of this erratum.

Sect. 2.4, third paragraph: $f_{\mathrm{s}}^{\mathrm{P}}(j,k)$ should be read as $f_{\mathrm{P}}^{\mathrm{I}}(j,k)$.

Sect. 2.4, fifth and sixth paragraphs: The corrected paragraphs are given below.

In the averaged spectrum $\bar{S}_k(f)$ the algorithm also searches the largest peak [denoted $f_p^{\mathrm{I}_a}(k)$] and $f_p^{\mathrm{II}_a}(k)$ defined as the nearest to $f_{\mathrm{R}}(k-1)$ inside the interval $\Omega_{\mathrm{R}}(k)$ which is at least larger than 85 % of $f_p^{\mathrm{I}_a}(k)$. At this time the reference frequency $f_{\mathrm{R}}(k)$ can be updated as:

$$f_{\mathrm{R}}(k) = \beta f_{\mathrm{R}}(k-1) + (1-\beta) f_p(k) \tag{21}$$

where $\beta$ denotes the forgetting factor and $f_p(k)$ is defined by

$$f_p(k) = \begin{cases} f_p^{\mathrm{II}_a}(k), & \exists f_p^{\mathrm{II}_a}(k) \\ f_p^{\mathrm{I}_a}(k), & \text{otherwise} \end{cases}. \tag{22}$$

Finally, estimated respiration rate $\hat{f}(k)$ is defined as:

$$\hat{f}(k) = \alpha \hat{f}(k-1) + (1-\alpha) f_p(k) \tag{23}$$

$$\alpha = \begin{cases} \alpha_2, & \exists f_p^{\mathrm{II}_a}(k) \\ \alpha_1, & \text{otherwise} \end{cases} \tag{24}$$

where $\alpha_2 \leq \alpha_1$, providing more memory when $f_p^{\mathrm{II}_a}(k)$ could not be set.

**Table 2** Percentage of utilization of each DR signal in combination of PRV, PAV and PWV

| Group | Percentage of use (%) | | |
|---|---|---|---|
| | PRV | PAV | PWV |
| $\bar{f}_{\mathrm{RES}} \geq 0.15$ Hz | 48.24 | 37.80 | 67.63 |
| $\bar{f}_{\mathrm{RES}} < 0.15$ Hz | 59.77 | 61.27 | 42.41 |
| All | 52.31 | 46.08 | 58.73 |

The online version of the original article can be found under doi:10.1007/s11517-012-0954-0.

J. Lázaro (✉) · E. Gil · R. Bailón · A. Mincholé · P. Laguna
Communications Technology Group (GTC), Aragón Institute of Engineering Research (I3A), IIS Aragón, Universidad de Zaragoza, Zaragoza, Spain
e-mail: jlazarop@unizar.es

J. Lázaro · E. Gil · R. Bailón · A. Mincholé · P. Laguna
Centro de Investigación Biomédica en Red en Bioingeniería, Biomateriales y Nanomedicina (CIBER-BBN), Zaragoza, Spain